On the partial wrinkling of imperfectly guided webs
(Supplementary online material)

Ciprian D. Coman[†]

School of Computing & Engineering,
University of Huddersfield, HD1 3DH, Huddersfield, UK

November 4, 2023

The material included below provides a number of additional details that complement the results reported in the main paper (referred to as CDC23[*] henceforth). The referencing of the equations in that work will be done by using their original labels; all numbers enclosed between square brackets included in this document correspond to the references listed at the back of CDC23.

We start off by first clarifying the morphological differences between the various localised eigenfunctions relative to their mode number $m \geq 1$ introduced in equation (2.3). This is shown in Figure 1 in the case of a localised eigenfunction $u \equiv u(y)$. It is re-iterated here that the mode number is typically identified as part of the solution, as explained in (2.7); this is a standard procedure widely used in many problems of stability (not just for plates or shells).

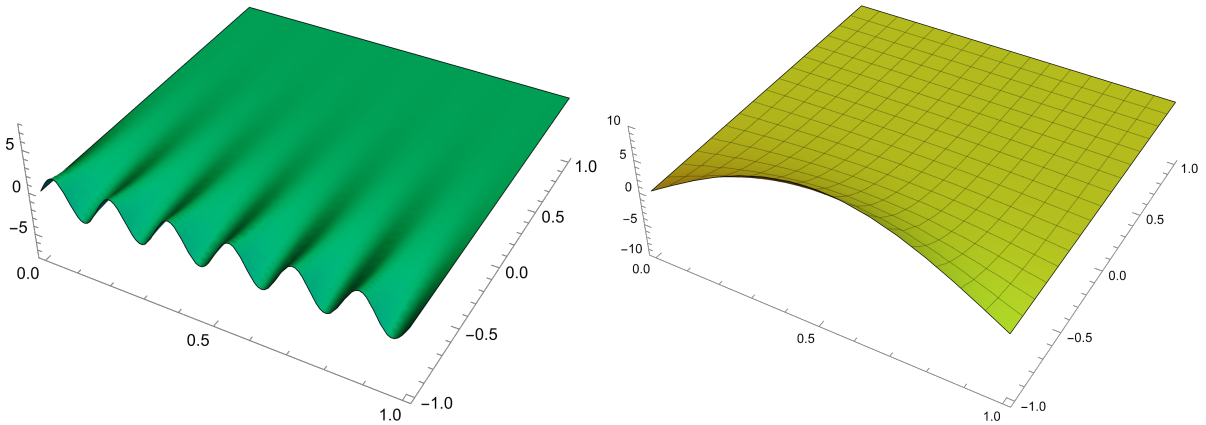

Figure 1: Illustrative *generic* examples of typical shapes of the instability patterns obtained from the boundary-value problem (2.1)-(2.2) in CDC23 for $\delta \neq 0$ and $\mu \gg 1$. These eigenmodes correspond to localised forms of $u(y)$ with $m = 1$ (right) or $m = 6$ (left). The latter deformation mode represents a particular instance of *partial wrinkling* (sometimes referred to as 'edge-buckling' for obvious reasons).

[†]cdc3p@yahoo.com

[*]Coman, C.D.: On the wrinkling of imperfectly guided webs, Mechanics Research Communications (submitted)

In Figure 2 of CDC23 it was shown that the response curves $\lambda \equiv \lambda(Q)$ related to the inhomogeneous case exhibited a global minimum, Q_c (say). The eigenmodes of (2.5)-(2.6) associated with a few of those minima are included in Figure 2; it is clear that the localisation experienced by these functions becomes more pronounced as μ increases. A somewhat similar localisation trend is also encountered for the homogeneous case, but in the limit $\beta \to 0^+$ with $\mu \gg 1$ fixed (this aspect was briefly touched upon in references [6] and [9] mentioned in CDC23 – e.g., see Figure 7 in [9]; a more detailed exploration of the case $0 < \beta \ll 1$ has been undertaken in our recent study [21]).

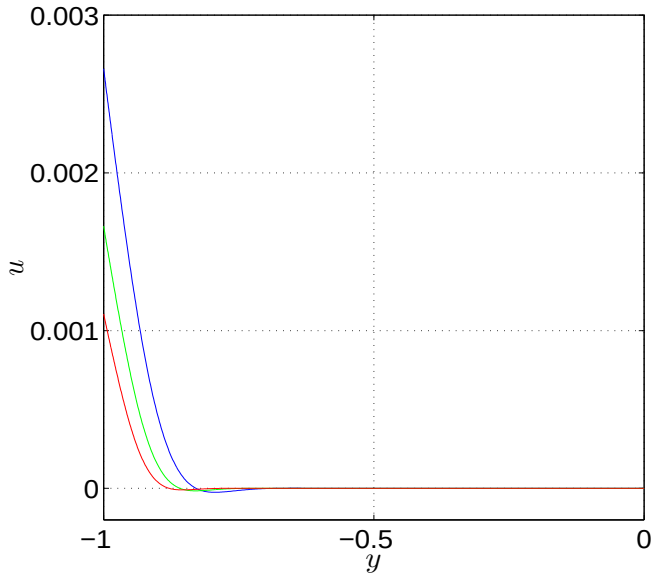

Figure 2: Samples of *critical* eigenmodes $u \equiv u(y)$ for the bifurcation equation (2.5)-(2.6) corresponding to the global minima of the curves in Fig. 2 of CDC23: $\mu = 600$ (blue), $\mu = 800$ (green), and $\mu = 1000$ (red). For clarity purposes, the horizontal range has been restricted to $[-1, 0]$ since the curves shown here are exponentially close to zero for $y \in [0, 1]$. All three functions are normalised so that their L_2-norm is 1.

The information that transpires from Figure 2 in CDC23 must be used in conjunction with the aspect ratio of the plate (i.e., β defined in (2.4a)). By way of example, we will consider the case of the response curve for $\mu = 1000$. In this case $Q_c \simeq 2.8 \times 10^{-4}$. According to the definition of Q in (2.4b), the critical mode number m_c can be expressed as $m_c = Q_c^{1/2}\mu\beta$, so for the particular situation considered here $m_c \simeq 16.73\beta$. Once a value of β has been chosen, one can find an approximation for the mode number by considering (for instance) the nearest positive integer to the value provided by this last formula. For instance, if $\beta = 1$ (e.g., $\ell = \pi$ and $b = 1$) then $m_c \simeq 17$, while for $\beta = 0.1$ (e.g., $\ell = \pi$ and $b = 10$) we obtain $m_c \simeq 2$. It must be emphasised that, unlike the related study [21], in the present investigation it is assumed that $\beta = \mathcal{O}(1)$. The same reasoning can be employed for other values of $\mu \gg 1$ (e.g., $Q_c \simeq 3.7 \times 10^{-4}$ for $\mu = 600$, and so on). If the predicted value of the mode number turns out to be $m_c < 1$, then one must take $m_c = 1$ (because the admissible values of this parameter are expected to obey $m \geq 1$).

To clarify how the mode number is identified in a general context, we have included in Figure 3 a pictorial description of the two possible scenarios at work when the response curves admit a global minimum for a $Q_c \neq 0$. It must be re-iterated that the re-scaled mode number $Q > 0$ is in fact a discrete quantity, so we write $Q_m := Q(m) \equiv m^2\beta^{-2}\mu^{-2}$ with $m = 1, 2, \ldots$. In practice it is

more convenient to treat Q as a continuous variable (and this is implied in the condition (2.7) stated in CDC23). Nevertheless, whichever method is preferred, the final results are similar as it will be explained shortly. In preparation for that we will introduce a few more notations. For each Q_m we get a unique $\lambda_m := \lambda(Q_m)$; examples of points (Q_m, λ_m) are shown as round (yellow) markers on the hypothetical (red) response curve in Figure 3. The position of these points relative to the global minimum (shown as the round (blue) marker) dictates what the mode number will be. For example, a possible scenario can be seen in the left sketch of Figure 3; this corresponds to the sequence Q_m $(m = 1, 2, \dots)$ "straddling" Q_c. The nearest neighbours of this latter point are Q_j and Q_{j+1} for some fixed $j \geq 1$. Another scenario is included in the right sketch of the same Figure. This time the sequence of points Q_m $(m = 1, 2, \dots)$ is situated to the right of Q_c, and the "nearest" neighbour is Q_1 (this need not be close to Q_c). With these preliminaries in mind, we can now formalise the identification of the mode number.

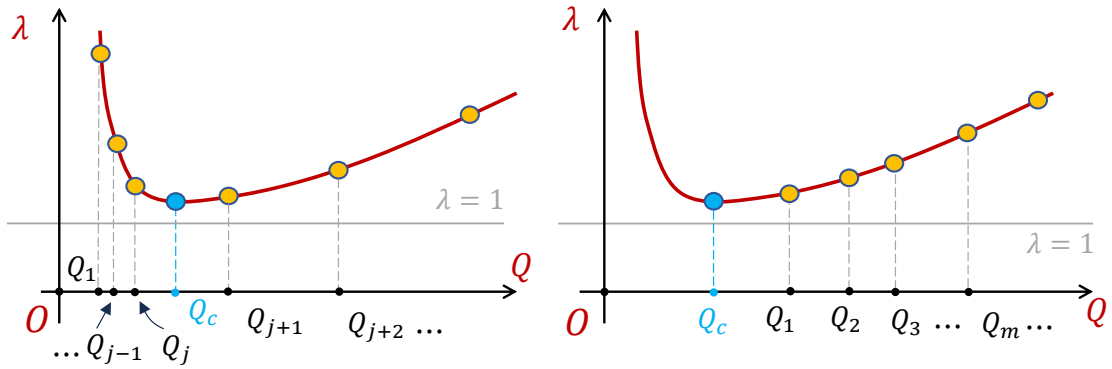

Figure 3: Two hypothetical situations for the identification of the *critical* mode number $m_c \in \mathbb{N}$ when the response curves admit a global minimum at $Q = Q_c$ (e.g., the scenario for the inhomogeneously tensioned web – see right window of Fig. 2 in CDC23).

It is convenient to slightly change the original notation for m_c. As explained above, once Q_c has been found (numerically) one can obtain an $m_c \in \mathbb{R}$; this will be denoted by m_c^* in what follows (it should be clear that $m_c^* \equiv Q_c^{1/2}\beta\mu$, as already mentioned). We can then define $m_c \in \mathbb{N}$ by

$$m_c := \begin{cases} j \text{ or } j+1\,, & \text{if} \quad j < m_c^* < j+1 \quad (j \geq 1)\,, \\ 1\,, & \text{if} \quad 0 < m_c^* < 1\,. \end{cases}$$

The first condition in the definition of m_c is unambiguous if some suitable conventions are adopted; if $\lambda_j > \lambda_{j+1}$ then $m_c = j + 1$, while for $\lambda_j < \lambda_{j+1}$ we choose $m_c = j$. In the exceptional case when $\lambda_j = \lambda_{j+1}$ we choose j if $m_c^* < j + (1/2)$ or $(j + 1)$ if the reverse is true. The situation $\lambda_j = \lambda_{j+1}$ and $m_c^* = j + (1/2)$ can be excluded right from the outset since the response curves cannot be symmetric in the inhomogeneous case ($\delta \neq 0$). Of course, if $m_c \gg 1$ – as it was the case for the situations $\delta = \mathcal{O}(1)$ or $\delta = \mathcal{O}(\delta^{-p})$ (with $0 < p < 2$) in §4 and §5 of CDC23, respectively, it does not really matter whether one chooses j or $(j + 1)$ for m_c; the errors introduced will be very small (also, in that case the points Q_m, with $m = 1, 2, \dots$, are closely spaced together). Even in the case $m_c = \mathcal{O}(1)$ one can simply choose the nearest positive integer to $m_c^* > 1$ without incurring very substantial errors.

For a given response curve (i.e., μ is fixed), the location of the points Q_m depends not only on $m = 1, 2, \ldots$, but also on the aspect ratio β. For strip-like configurations (i.e., $\ell > \pi b$), as β increases the points Q_m will shift towards the vertical λ-axis. This means that in this case Q_1 will end up to the left of Q_c for a sufficiently large β; in other words, $m_c > 1$. By contrast, for web-like configurations β tends to be on the small side (in the numerical results of Banichuk *et al.* mentioned in CDC23, $\beta \simeq 6 \times 10^{-2}$). In this scenario the sequence of points Q_m will migrate in the positive direction of the Q-axis as β gets smaller, so there is a chance that for a sufficiently small β all the points in this sequence will end up to the right of Q_c. Under these conditions it is clear that the critical mode number is $m_c = 1$ because $\lambda_1 < \lambda_2 < \cdots < \lambda_m < \lambda_{m+1} < \ldots$ and $\lambda_c \simeq \min\{\lambda_k \mid k = 1, 2, \ldots\}$; we refer to the right sketch in Figure 3 for a visual depiction of such a scenario.

For the remaining of this discussion we will amplify some of the brief remarks/statements made in §3 of CDC23, in relation to the homogeneous case ($\delta = 0$). The situation for this scenario is very simple because (2.5) reduces to an ODE with constant coefficients which admits a closed-form solution. As explained in reference [8], the solutions of that equation can be split into two groups characterised by their symmetry or anti-symmetry relative to $y = 0$. It was established in the same place that the critical eigenvalue of the boundary-value problem (2.5)-(2.6) is associated with the symmetric mode. This observation allows us to restrict the integration range to $y \in [-1, 0]$, provided that we also enforce the symmetry conditions $u' = u''' = 0$ at $y = 0$. By introducing the new quantity $\overline{Q}^2 := \mu^2 Q = (m/\beta)^2$ ($\overline{Q} > 0$) the bifurcation problem becomes

$$
\begin{aligned}
&u'''' - 2\overline{Q}^2 u'' + \overline{Q}^2\big[\overline{Q}^2 + \mu^2(1-\lambda)\big]u = 0\,, \qquad -1 < y < 0\,,\\
&u'' - \nu\overline{Q}^2 u = 0\,, \qquad u''' - (2-\nu)\overline{Q}^2 u' = 0\,, \qquad y = -1\,,\\
&u' = u''' = 0\,, \qquad y = 0\,.
\end{aligned}
$$

We will refer to this problem as (BVP0). Although these equations are slightly different from those discussed in [9], the method of solution for (BVP0) remains the same. We include below some details that establish the validity of this assertion (in order to clarify some objections raised by one of the anonymous reviewers).

By writing

$$\lambda = 1 + \gamma^2\overline{Q}^2\mu^{-2}\,, \qquad (\gamma \in \mathbb{R})\,,$$

the ODE in (BVP0) becomes

$$u'''' - 2\overline{Q}^2 u'' + \overline{Q}^4\big(1-\gamma^2\big)u = 0\,.$$

The parameter γ plays the role of the new eigenvalue in the transformed version of (BVP0). Since the characteristic roots of this last equation are $\pm\overline{Q}\sqrt{1 \pm \gamma}$, it is clear that one has to consider separately the possibility that either $|\gamma| < 1$ or $|\gamma| > 1$ – the vertical bars used here represent the absolute value of the quantity they enclose. In fact, it suffices to restrict our attention to either $0 < \gamma < 1$ or $\gamma > 1$. In reference [9] it is shown that the critical eigenvalue is associated with the former case; in our recent study [21] the higher points in the spectrum of (BVP0) – that is, those associated with $\gamma > 1$, are also discussed in some detail. Based on this existing body of work we can then confine our attention to $\gamma \in (0, 1)$. For this choice, the general *symmetric* solution of (BVP0) will be of the form

$$
\begin{aligned}
u(y) &= C_1 \cosh(\kappa_1 y) + C_2 \cosh(\kappa_2 y)\,,\\
\kappa_1 := \overline{Q}\sqrt{1-\gamma} \qquad &\text{and} \qquad \kappa_2 := \overline{Q}\sqrt{1+\gamma}\,,
\end{aligned}
$$

for some arbitrary constants C_1, $C_2 \in \mathbb{R}$; these constants will be identified from the boundary conditions stated above. Note that the above proposed expression of $u(y)$ already satisfies the appropriate symmetry conditions.

An important observation in relation to the above developments is that the characteristic roots are independent of $\mu \gg 1$, so we expect the shape of the critical eigenmodes of (BVP0) to be insensitive to variations in that quantity. Another feature that can be anticipated is related to the size of λ; this is expected to be close to 1 (as clearly demonstrated by the numbers on the vertical axis in the left window of Figure 2 in CDC23).

Enforcing the aforementioned boundary conditions leads to the determinantal equation

$$\kappa_1 \sinh(\kappa_1)\cosh(\kappa_2)(1+\gamma-\nu)^2 = \kappa_2 \sinh(\kappa_2)\cosh(\kappa_1)(1-\gamma-\nu)^2 \,.$$

For each given value $0 < \nu < 0.5$ this transcendental equation can be routinely solved numerically to obtain the dependence $\gamma \equiv \gamma(\overline{Q})$, which can eventually help us find a graphical representation for the response curves $\lambda \equiv \lambda(\overline{Q})$ (e.g., see Figure 2 of CDC23). Using standard computational tools (e.g., arc-length continuation) we have employed the determinantal equation to compute the γ versus $\overline{Q}$ curves mentioned above; the corresponding results for a small sample of Poisson's ratios ($\nu \in \{0.1, 0.3, 0.5\}$) are shown in Figure 4. Finally, the dependence of λ on $\overline{Q}$ is illustrated in Figure 5 for $\nu = 0.3$ and $\mu \in \{800, 1000, 1200\}$. These results are compared with the direct numerical simulations of the solutions of (BVP0), which are also included in CDC23; as expected, the two sets of results match perfectly.

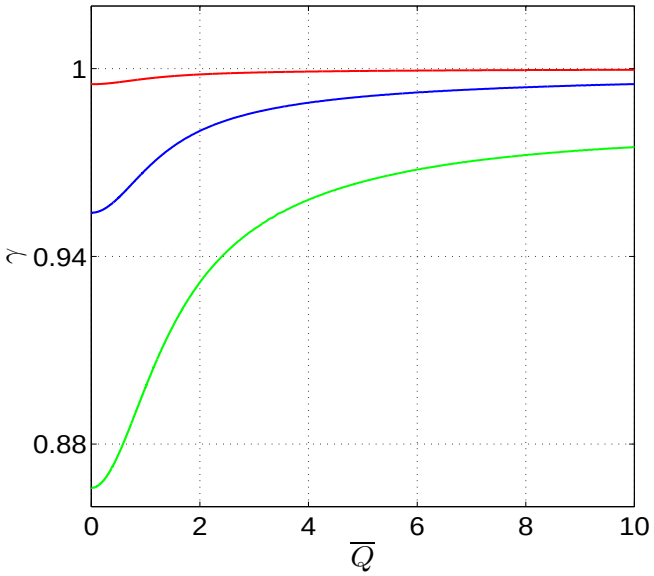

Figure 4: Examples of curves $\gamma \equiv \gamma(\overline{Q})$ obtained from the exact determinantal equation for the *homogeneous* case ($\delta = 0$); $\nu = 0.1$ (red), $\nu = 0.3$ (blue), and $\nu = 0.5$ (green).

The discussion about the identification of the critical mode number included in the earlier part of this document can be trivially extended to the homogeneous case ($\delta = 0$). The response curves $\lambda = \lambda(\overline{Q})$ are monotonic increasing and admit a global minimum at $(\overline{Q}, \lambda) = (0, 1)$. The increasing sequence of points $\overline{Q}_m := (m/\beta)^2$ will always yield another increasing sequence $\lambda_m := \lambda(\overline{Q}_m)$, so the

minimum energy configuration of the buckled web corresponds to the point $(\overline{Q}_1, \lambda_1)$. The changes in μ have no effect on the monotonicity properties of the response curves. Decreasing $\beta > 0$ results in a shift of the points $\overline{Q}_m$ in the positive direction of the $\overline{Q}$-axis. As shown in [21], as $\beta \to 0^+$ the critical eigenmode becomes progressively localised near $y = -1$ and has a somewhat similar visual appearance to the samples recorded in Figure 2 (but these localised forms are mathematically quite distinct).

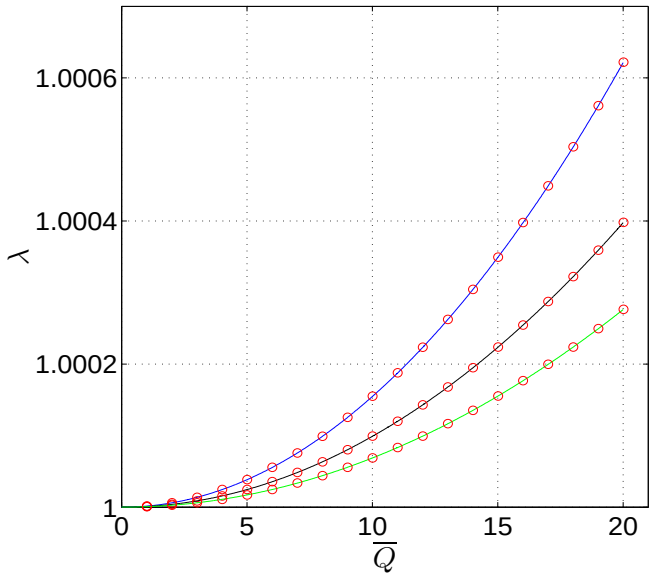

Figure 5: Response curves obtained from the data in Fig. 4 for $\nu = 0.3$ and $\mu = 800$ (blue), $\mu = 1000$ (black), $\mu = 1200$ (green). The superimposed red markers correspond to the direct numerical solution of the bifurcation problem (2.5)-(2.6) in CDC23; these latter results are also included in the left window of Fig. 2 in the same place (but for a bigger $\overline{Q}$-range.)